COMMUNICATIONS

Dynamics of the $O(^1D)+CO_2$ oxygen isotope exchange reaction

Mark J. Perri and Annalise L. Van Wyngarden
Department of Chemistry, University of California, Berkeley, California 94720-1460

Kristie A. Boering[a)]
Department of Chemistry and Department of Earth and Planetary Science, University of California, Berkeley, California 94720-1460

Jim J. Lin
Institute of Atomic and Molecular Science, Academia Sinica, Taipei, Taiwan 106

Yuan T. Lee
Institute of Atomic and Molecular Science, Academia Sinica, Taipei, Taiwan 106 and Department of Chemistry, National Taiwan University, Taipei, Taiwan

(Received 1 July 2003; accepted 25 August 2003)

The $^{18}O(^1D)+^{44}CO_2$ oxygen isotope exchange reaction has been studied using a crossed molecular beam apparatus at a collision energy of 7.7 kcal/mol. Two different reaction channels are observed, both proceeding via a relatively long-lived CO_3 complex. Electronic quenching of $O(^1D)$ is the major channel, accounting for 68% of all isotope exchange, while 32% occurs without quenching. These results are the first experimental evidence that isotope exchange can occur through a long-lived CO_3 intermediate without subsequent crossing to the triplet surface, and could prove important for atmospheric models of oxygen isotope exchange between CO_2 and O_3. [DOI: 10.1063/1.1618737]

Stratospheric CO_2 is enriched in the stable heavy isotopes ^{17}O and ^{18}O relative to tropospheric CO_2,[1] but a quantitative, molecular-level understanding of the enrichment is lacking. The enrichments are anomalous (or "mass-independent") since the enrichment in ^{17}O is greater than that in ^{18}O, while standard equilibrium and kinetic isotope effects result in changes in ^{17}O only half as large as those for ^{18}O when measured relative to the major isotope ^{16}O.[2] Atmospheric ozone is also anomalously enriched[3] in ^{17}O and ^{18}O due to unusual isotope effects in the 3-body recombination reaction (R1),[4]

$$O(^3P)+O_2+M\rightarrow O_3^*+M\rightarrow O_3+M^*. \quad \text{(R1)}$$

Gao and Marcus,[5] using a semiempirical RRKM approach, suggested that the anomalous enrichment in O_3 in the atmosphere is primarily due to subtle, nonstandard differences in the densities of states between symmetric and asymmetric isotopologues (e.g., $^{16}O^{16}O^{16}O$ versus $^{18}O^{16}O^{16}O$). For the case of CO_2, it was suggested[6,7] that the anomalous oxygen isotopic composition of O_3 could be transferred to CO_2 by photolysis of O_3 to form $O(^1D)$ (R2) followed by a quenching collision between $O(^1D)$ and CO_2 in which isotopic exchange can occur (R3):

$$O_3+h\nu\rightarrow O(^1D)+O_2 \quad \lambda<340\ \text{nm}, \quad \text{(R2)}$$

$$O(^1D)+CO_2\rightarrow CO_3^*\rightarrow O(^3P)+CO_2 \quad \text{(R3)}$$

$$\Delta E=-46\ \text{kcal/mol}.$$

[a)]Author to whom correspondence should be addressed. Electronic mail: boering@cchem.berkeley.edu

This idea was based on earlier laboratory work demonstrating isotope exchange between ^{18}O-labeled CO_2 and $O(^1D)$ in which $O(^1D)$ was generated by photolysis of O_3,[8,9] N_2O,[10] NO_2,[11] or CO_2.[12] To date, however, models of isotope exchange between CO_2 and O_3 in the stratosphere and in bulk photochemical experiments have been unable to reproduce the observed enrichments.[6,13] Thus, it is not known whether there is an additional anomalous isotope effect in the $O(^1D)+CO_2$ reaction or whether transfer of the isotope anomaly from O_3 via (R2) and (R3) is sufficient. Resolving these uncertainties is not only of interest from a chemical physics perspective but also has environmental applications. For example, observations of the anomalous isotopic composition of CO_2 may provide a unique tracer of stratospheric chemistry and transport on time scales of months to years[14] and a means to quantify gross carbon fluxes to and from the biosphere on annual[15] to millennial[16] time scales if the mechanisms for isotope exchange are understood.

The kinetics of the quenching of $O(^1D)$ by CO_2 has received considerable attention, but little direct information on the dynamics is known. The quenching reaction is unusual in that it is spin-forbidden but proceeds at a nearly gas kinetic rate of $1.1\times10^{-10}\ \text{cm}^3\ \text{s}^{-1}$,[17] while reaction to form $CO+O_2(^1\Sigma_g^+, ^1\Delta_g, ^3\Sigma_g^-)$ proceeds at a rate of only $2.4\times10^{-13}\ \text{cm}^3\ \text{s}^{-1}$ when the reactant $O(^1D)$ is produced by room temperature photolysis of N_2O.[18] The bulk isotope exchange experiments of the 1960s[8–12] are consistent with formation of a relatively long-lived collision complex, CO_3^*, in which both isotope exchange and curve-crossing from the triplet to the singlet surface can occur. DeMore and Dede[19] inferred a CO_3^* lifetime of 1 to 10 ps from the pressure dependence of CO_3 formation at high pressures in the gas phase. The isotope labeling results of Baulch and Breckenridge[12] suggest a near-statistical rate of isotope exchange for which the incoming $O(^1D)$ atom has an approximately 2/3 chance of being incorporated into the product CO_2 molecule. Such a statistical exchange is consistent with a D_{3h} structure for the CO_3 complex or a C_{2v} structure which can access the D_{3h} structure during the CO_3^* lifetime. IR spectroscopy of CO_3 formed in solid CO_2 and Ar matrices suggests that the C_{2v} structure is more stable at low temperatures.[9,20] The most recent *ab initio* calculations suggest that the C_{2v} geometry is more stable than D_{3h} by 4.0 kcal/mol and that the barrier between them is relatively small.[21] If this is correct, the longer the CO_3^* lifetime, the more chance the complex has to sample the symmetric D_{3h} geometry. In addition, the longer the lifetime, the more complete intramolecular vibrational energy redistribution (IVR) will be. Both these effects would serve to increase the probability that all oxygen atoms are equivalent on the time scale of the collision complex lifetime and possess an equal chance of becoming the product oxygen atoms. No studies have been performed to date, however, under single collision conditions in which the dynamics of the isotope exchange and quenching in (R3) can be studied. Single collision conditions are particularly important in this case since the formation of ozone in bulk photochemical experiments may complicate isotopic results due to the large and anomalous isotope effects in (R1).

To investigate the dynamics of the $CO_2+O(^1D)$ reaction, we have used an improved universal crossed molecular beam apparatus.[22] In this experiment, a beam of $^{18}O(^1D)$ is crossed with a beam of $^{44}CO_2$, and the time-of-flight of the resulting isotope exchange product, $^{46}CO_2$, is detected. Two product channels for isotope exchange are observed: one in which the products have considerably more translational energy than the collision energy and one in which the maximum translational energy of the products is equal to the collision energy. We, therefore, attribute these two channels to isotope exchange in quenching and nonquenching collisions, respectively.

The atomic beam of 50% $^{18}O(^1D)$ and 50% $^{18}O(^3P)$ was generated by 157.6 nm photolysis of doubly labeled $^{36}O_2$ with an isotopic purity greater than 95% as verified by mass spectrometry. The ^{18}O reactant was used to avoid background from the reactant $^{44}CO_2$ beam and to ensure all products detected had undergone reaction and not inelastic scattering with the oxygen atom beam. In addition, a copper cold plate cooled by a closed cycle He-cryocooler is located in the main chamber where the beams emerge from the source chambers. This cold plate was maintained at approximately 20 K and dramatically reduces the ambient CO_2 background in the chamber.

The O_2 beam was produced from a tuned pulsed valve (General Valve) with an approximate rise time of 50 μs and a backing pressure between 60 and 80 psig. The pulsed valve was rotated approximately 90° to the reaction plane to reduce background O_2 gas in the main chamber. The photolysis laser (Lambda Physik LPX 210 F_2 laser), with a power of 60 mJ per pulse at a 50 Hz repetition rate, was focused with a

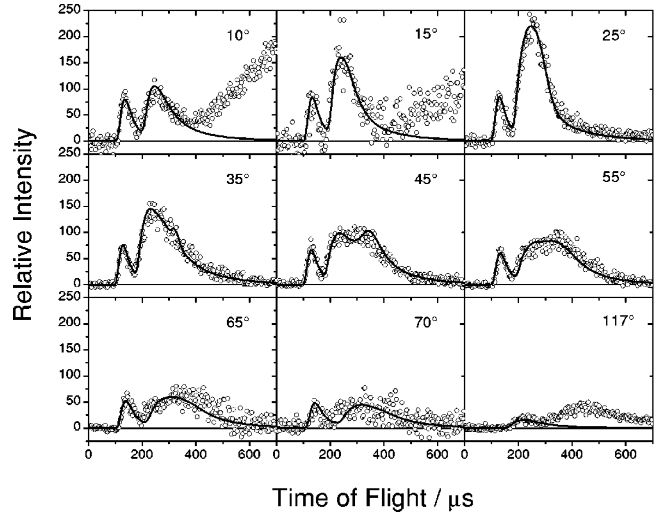

FIG. 1. Mass 46 time-of-flight data. The angles displayed are in the laboratory frame. Raw data are represented by open circles, and the simulations are shown as lines.

spherical-cylindrical MgF_2 lens to a spot size of 3×4 mm. At this power, the O_2 transition is saturated. The laser crossed the O_2 beam just after the skimmer, and the $O(^1D)$ was skimmed by another 4 mm skimmer. In this setup, the mean velocity of $^{18}O(^1D)$ is 2155±10 m/s with a speed ratio of 27 and an angular divergence of ±4°.

To form a molecular beam of CO_2, a mixture of 33% CO_2 (99.99%) in Ar (99.999%) was used at low pressures (6 psig) to reduce the formation of clusters. The Ar also served to increase the speed ratio of the beam. The gas mixture was run through a tuned pulsed valve (General Valve) similar to the O_2 source and skimmed with a 1.5 mm diameter skimmer. The average CO_2 beam speed was 620±5 m/s with a speed ratio of 11 and angular divergence of ±3°. With these speeds, the collision energy is 7.65±0.1 kcal/mol.

After the beams cross, the neutral products travel a distance of 247 mm to the detector, where they are ionized by electron impact. The product ions which have undergone isotope exchange ($^{46}CO_2$) are mass selected by a quadrupole mass filter and directed to a Daly detector. Time-of-flight spectra are then acquired by a multichannel scaler with a 1 μs bin size. The detector is attached to the top flange of the main chamber which can be rotated about the beam crossing point from −35° to 125°, with the $O(^1D)$ beam defined as 0°. However, the full range of the detector was not used in this experiment due to the higher background generated close to the beam directions. The angles studied range from 10° to 70° with an additional measurement at 117°. As the detector was rotated closer to 0°, the $^{46}CO_2$ background rose sharply due to O-atom exchange on the surface of the cold plate. At angles near 90°, the normal isotopic abundance of $^{46}CO_2$ in the beam gives rise to a high background. Despite these limitations, the laboratory angles measured cover almost the entire range of center-of-mass angles relevant for this study.

The raw time-of-flight data for mass 46 products are shown in Fig. 1. There are two distinct peaks, a fast peak with an average flight time of 130 μs at a laboratory angle of

TABLE I. Branching ratios and product translational energies.

Reaction	Branching	$\langle E_t \rangle$	f[a]
$^{18}O(^1D)+^{44}CO_2 \rightarrow ^{16}O(^3P)+^{46}CO_2$	68%	27.1 kcal/mol	50%
$^{18}O(^1D)+^{44}CO_2 \rightarrow ^{16}O(^1D)+^{46}CO_2$	32%	3.1 kcal/mol	60%

[a] $f=E_{int}/(E_t+E_{int})$

45° and a slower, broader peak centered at approximately 280 μs at 45°. Note that the extra background mentioned above is apparent at 10° and 15° as a rise in signal around 400 μs, while at 117° it appears as an extra peak centered at 450 μs due to the physical geometry of the main chamber. The backing pressure dependence of the CO_2 beam has been checked to ensure that both the fast and slow peaks are from collisions of CO_2 monomers with oxygen atoms. Because only mass 46 is detected, both the fast and slow channels observed must correspond to isotope exchange. Moreover, since the barrier for any possible isotope exchange between $O(^3P)$ and CO_2 is predicted to be approximately 34 kcal/mol,[21] and earlier bulk isotope exchange studies showed no exchange between $O(^3P)$ and CO_2,[8,10] both peaks observed presumably correspond to two different $O(^1D)+CO_2$ channels.

In order to extract center-of-mass product speed and angular information from the raw data, computer simulations were performed. Initial guesses for the center-of-mass product kinetic energy distribution, P(E), and the center-of-mass product angular distribution, $P(\theta)$, were input into an iterative forward-convolution computer program, along with the beam and machine parameters. Laboratory-frame time-of-flight spectra were generated from these inputs and compared with the experimental data, which were rebinned to 3 μs to improve the signal-to-noise ratio. Values of P(E) and $P(\theta)$ for each channel were then iteratively adjusted to get a satisfactory fit to the raw data, yielding the solid curves in Fig. 1. The only lab angle which was not fit well is 70°, which contains a third peak at 215 μs due to scattering of $^{46}CO_2$ present at natural abundance in the 90° beam. This effect will be corrected for in a later paper which will also describe a redesigned source to achieve a lower collision energy.

The product translational energies for both channels are summarized in Table I. For the fast peak, a broad P(E) was used with a maximum energy of 53.7 kcal/mol. Since the average product translational energy for this fast channel is 27.1 kcal/mol, which is much greater than the collision energy, it was assigned to the quenching reaction (R3). Out of the available energy of 53.7 kcal/mol, this leaves 50% for internal excitation of the product $^{46}CO_2$. This value is consistent with a previous flow tube study which used a higher collision energy of 13.0 kcal/mol; by measuring the product $O(^3P_2)$ Doppler profile at 130.2 nm, it was found that $49\pm3\%$ of the available energy was deposited into the product CO_2.[23]

The slow peak, with $\langle E_t \rangle = 3.1$ kcal/mol, was also fit with a broad P(E). The maximum translational energy of this channel is 7.7 kcal/mol, equal to the collision energy. This peak therefore corresponds to isotope exchange without quenching (R4),

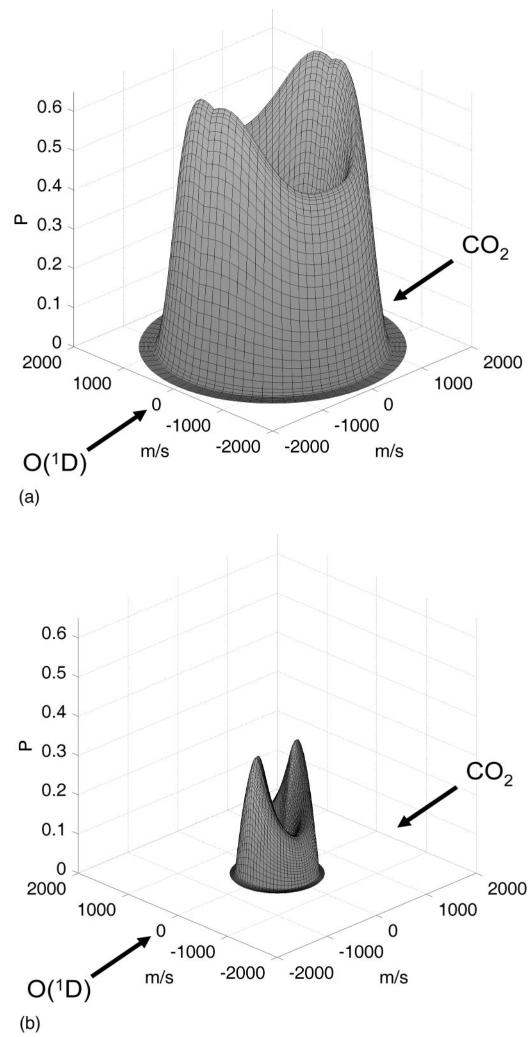

FIG. 2. The 3D center-of-mass product velocity flux diagram obtained from the simulated P(E) and $P(\theta)$ distributions for (a) the $^{46}CO_2$ product in the quenching isotope exchange channel (the fast peak in Fig. 1) and (b) the $^{46}CO_2$ product in the nonquenching isotope exchange channel (the slow peak in Fig. 1). The probabilities have been normalized by the branching ratio of each channel.

$$^{18}O(^1D)+^{44}CO_2 \rightarrow CO_3^* \rightarrow ^{16}O(^1D)+^{46}CO_2. \qquad (R4)$$

This result is the first observation of isotope exchange on the singlet surface leading to singlet products, as no previous experiment that monitored isotope exchange could also determine the electronic state of the product oxygen atom. This channel is significant, accounting for 32% of all isotope exchange. Similar to the quenching channel, 60% of the available energy was deposited into the product CO_2.

Together with the P(E) values described above, the derived values for $P(\theta)$ in (R3) and (R4) are graphed as product velocity flux diagrams ($d\sigma/du \sin\vartheta d\vartheta$) in Fig. 2. Both channels clearly show forward-backward symmetry which indicates that both involve an intermediate with a lifetime greater than its rotational period. No evidence for a direct isotope exchange mechanism is observed for either channel. We note that since the nonquenching peak at the laboratory angle of 70° (180° in the center-of-mass frame) could not be fit by simulation, the $P(\theta)$ for the nonquenching channel is not as accurate in the backward scattered region. However, because the 180° center-of-mass angle is covered by other laboratory angles, the inaccuracy in $P(\theta)$ for the nonquenching peak should be small. Additionally, the most important angles for the branching ratio determination are from 45° to 135° in the center-of-mass frame, which covers 70% of the full solid angle (4π).

Although this experimental technique confirms the role of a relatively long-lived intermediate in both the quenching and nonquenching channels, it can only give a lower bound for the CO_3 complex lifetime of approximately a few rotational periods. Theoretical studies are needed to determine the effect of lifetime on energy partitioning, which could lead to additional isotope effects for this reaction. If IVR is fast such that energy randomization takes place within the complex lifetime, and if a symmetric CO_3 structure is accessed, then each oxygen atom may have an equal probability (ignoring any zero point energy effects) of being ejected and becoming the product oxygen atom. If IVR is slow and energy redistribution does not occur during the CO_3 complex lifetime, then there may be a preference for the incoming oxygen atom to also be the product oxygen atom.

In summary, two reaction channels for isotope exchange from collisions of $O(^1D)$ and CO_2 have been observed using a crossed molecular beam technique. The fast channel is attributed to the expected $O(^1D)$ to $O(^3P)$ quenching reaction. The observation of a slow channel provides the first experimental evidence that isotope exchange can occur through a relatively long-lived CO_3 intermediate without crossing to the triplet surface. For atmospheric applications, the branching ratios of the two channels should be investigated at collision energies corresponding to reactions in the stratosphere, approximately 1 to 1.5 kcal/mol.[24] A future paper will report on results using a redesigned O_2 source which can achieve much slower $O(^1D)$ speeds. It is expected that the branching ratio of the nonquenching channel will decrease as the collision energy is lowered, since the CO_3^* lifetime should increase. A longer lifetime will allow more opportunities for intersystem crossing to occur, thereby increasing the probability of quenching. If the previously ignored nonquenching channel is still significant at lower collision energies, then models of the oxygen isotope anomaly may need to take this isotope exchange mechanism into account. The potential impacts of this nonquenching channel on model predictions of the CO_2 isotopic composition in the stratosphere and on interpretations of previous laboratory experiments are currently under investigation.

This research was supported by the U.S. National Science Foundation Atmospheric Chemistry Program (ATM-0096504); by Academia Sinica, Taiwan; by a National Science Foundation Predoctoral Fellowship for AV; and by the David and Lucile Packard Foundation (KAB). M.P. and A.V. thank M. Ahmed for early help in studying this reaction.

[1] T. Gamo, M. Tsutsumi, H. Sakai, T. Nakazawa, M. Tanaka, H. Honda, H. Kubo, and T. Itoh, Tellus, Ser. B **41**, 127 (1989); M. H. Thiemens, T. Jackson, K. Mauersberger, B. Schueler, and J. Morton, Geophys. Res. Lett. **18**, 669 (1991); M. H. Thiemens, T. Jackson, E. C. Zipf, P. W. Erdman, and C. Vanegmond, Science **270**, 969 (1995); M. H. Thiemens, T. L. Jackson, and C. A. M. Brenninkmeijer, Geophys. Res. Lett. **22**, 255 (1995); B. Alexander, M. K. Vollmer, T. Jackson, R. F. Weiss, and M. H. Thiemens, *ibid.* **28**, 4103 (2001); P. Lammerzahl, T. Rockmann, C. A. M. Brenninkmeijer, D. Krankowsky, and K. Mauersberger, *ibid.* **29**, doi: 10.1029/2001GL014343 (2002).
[2] See, e.g., M. H. Thiemens, Science **283**, 341 (1999).
[3] K. Mauersberger, Geophys. Res. Lett. **14**, 80 (1987); B. Schueler, J. Morton, and K. Mauersberger, *ibid.* **17**, 1295 (1990); D. Krankowsky, P. Lammerzahl, and K. Mauersberger, *ibid.* **27**, 2593 (2000).
[4] K. Mauersberger, B. Erbacher, D. Krankowsky, J. Gunther, and R. Nickel, Science **283**, 370 (1999).
[5] Y. Q. Gao and R. A. Marcus, Science **293**, 259 (2001); Y. Q. Gao and R. A. Marcus, J. Chem. Phys. **116**, 5913 (2002); Y. Q. Gao, W. C. Chen, and R. A. Marcus, *ibid.* **117**, 1536 (2002).
[6] Y. L. Yung, A. Y. T. Lee, F. W. Irion, W. B. DeMore, and J. Wen, J. Geophys. Res. **102**, 10857 (1997).
[7] Y. L. Yung, W. B. Demore, and J. P. Pinto, Geophys. Res. Lett. **18**, 13 (1991).
[8] D. Katakis and H. Taube, J. Chem. Phys. **36**, 416 (1962).
[9] E. Weissberger, W. H. Breckenridge, and H. Taube, J. Chem. Phys. **47**, 1764 (1967).
[10] H. Yamazaki and R. J. Cvetanovic, J. Chem. Phys. **40**, 582 (1964).
[11] K. F. Preston and R. J. Cvetanovic, J. Chem. Phys. **45**, 2888 (1966).
[12] D. L. Baulch and W. H. Breckenridge, Trans. Faraday Soc. **62**, 2768 (1966).
[13] J. Wen and M. H. Thiemens, J. Geophys. Res. **98**, 12801 (1993); V. Barth and A. Zahn, *ibid.* **102**, 12995 (1997); J. C. Johnston, T. Rockmann, and C. A. M. Brenninkmeijer, *ibid.* **105**, 15213 (2000).
[14] K. A. Boering, EOS Trans. Am. Geophys. Union **83**, (2002), Fall Meet. Suppl., Abstract B61D-05.
[15] K. J. Hoag, K. A. Boering, C. J. Still, I. Y. Fung, and J. T. Randerson, EOS Trans. Am. Geophys. Union **83**, (2002), Fall Meet. Suppl., Abstract B71A-0707.
[16] B. Luz, E. Barkan, M. L. Bender, M. H. Thiemens, and K. A. Boering, Nature (London) **400**, 547 (1999); T. Blunier, B. Barnett, M. L. Bender, and M. B. Hendricks, Global Biogeochem. Cycles **16**, doi: 10.1029/2001GV001460 (2002).
[17] J. A. Davidson, C. M. Sadowski, H. I. Schiff, G. E. Streit, C. J. Howard, D. A. Jennings, and A. L. Schmeltekopf, J. Chem. Phys. **64**, 57 (1976); G. E. Streit, C. J. Howard, A. L. Schmeltekopf, J. A. Davidson, and H. I. Schiff, *ibid.* **65**, 4761 (1976); S. P. Sander, B. J. Finlayson-Pitts, R. R. Friedl *et al.*, Jet Propulsion Laboratory, Pasadena, JPL Publication 02-25 (2002).
[18] A. J. Sedlacek, D. R. Harding, R. E. Weston, T. G. Kreutz, and G. W. Flynn, J. Chem. Phys. **91**, 7550 (1989).
[19] W. B. DeMore and C. Dede, J. Phys. Chem. **74**, 2621 (1970).
[20] N. G. Moll, D. R. Clutter, and W. E. Thompson, J. Chem. Phys. **45**, 4469 (1966); M. E. Jacox and D. E. Milligan, *ibid.* **54**, 919 (1971).
[21] R. D. J. Froese and J. D. Goddard, J. Phys. Chem. **97**, 7484 (1993).
[22] J. J. Lin, D. W. Hwang, S. Harich, Y. T. Lee, and X. M. Yang, Rev. Sci. Instrum. **69**, 1642 (1998).
[23] Y. Matsumi, Y. Inagaki, G. P. Morley, and M. Kawasaki, J. Chem. Phys. **100**, 315 (1994).
[24] K. Takahashi, N. Taniguchi, Y. Sato, and Y. Matsumi, J. Geophys. Res. **107**, doi: 10.1029/2001JD001270 (2002).